01 Feb 2019

Raman Spectroscopy as a Predictive Tool for Monitoring Osteoporosis Therapy in a Rat Model of Postmenopausal Osteoporosis

J. Renwick Beattie

Antonia Sophocleous

M. Clare Caraher

Olive O'Driscoll

et. al. For a complete list of authors, see https://scholarsmine.mst.edu/che_bioeng_facwork/1083

CrossMark

Original Research

Raman spectroscopy as a predictive tool for monitoring osteoporosis therapy in a rat model of postmenopausal osteoporosis

J. Renwick Beattie[1] · Antonia Sophocleous[2] · M. Clare Caraher[3,4] · Olive O'Driscoll[5] · Niamh M. Cummins[6] · Steven E. J. Bell[4] · Mark Towler[7] · Alireza Rahimnejad Yazdi[7] · Stuart H. Ralston[8] · Aymen I. Idris[9]

Abstract

Pharmacological therapy of osteoporosis reduces bone loss and risk of fracture in patients. Modulation of bone mineral density cannot explain all effects. Other aspects of bone quality affecting fragility and ways to monitor them need to be better understood. Keratinous tissue acts as surrogate marker for bone protein deterioration caused by oestrogen deficiency in rats. Ovariectomised rats were treated with alendronate (ALN), parathyroid hormone (PTH) or estrogen (E2). MicroCT assessed macro structural changes. Raman spectroscopy assessed biochemical changes. Micro CT confirmed that all treatments prevented ovariectomy-induced macro structural bone loss in rats. PTH induced macro structural changes unrelated to ovariectomy. Raman analysis revealed ALN and PTH partially protect against molecular level changes to bone collagen (80% protection) and mineral (50% protection) phases. E2 failed to prevent biochemical change. The treatments induced alterations unassociated with the ovariectomy; increased beta sheet with E2, globular alpha helices with PTH and fibrous alpha helices with both ALN and PTH. ALN is closest to maintaining physiological status of the animals, while PTH (comparable protective effect) induces side effects. E2 is unable to prevent molecular level changes associated with ovariectomy. Raman spectroscopy can act as predictive tool for monitoring pharmacological therapy of osteoporosis in rodents. Keratinous tissue is a useful surrogate marker for the protein related impact of these therapies.The results demonstrate utility of surrogates where a clear systemic causation connects the surrogate to the target tissue. It demonstrates the need to assess broader biomolecular impact of interventions to examine side effects.

✉ Mark Towler
  mtowler@ryerson.ca

1 J Renwick Beattie Consulting, Causeway Enterprise Agency, Ballycastle, UK

2 Department of Life Sciences, European University Cyprus, Nicosia, Cyprus

3 ICON plc, South County Business Park, Leopardstown, Dublin, Ireland

4 School of Chemistry and Chemical Engineering, Queen's University Belfast, Stranmillis Road, Belfast, UK

5 AventaMed, Rubicon Centre, Rossa Avenue, Bishopstown, Cork, Ireland

6 Centre for Interventions in Infection, Inflammation and Immunity, Graduate Entry Medical School, University of Limerick, Limerick, Ireland

7 Department of Mechanical and Industrial Engineering, Ryerson University, Toronto, ON, Canada

8 Rheumatology and Bone Diseases Unit, Centre for Genomic and Experimental Medicine, MRC Institute of Genetics and Molecular Medicine, Western General Hospital, University of Edinburgh, Edinburgh, UK

9 Department of Oncology and Metabolism, Medical School, University of Sheffield, Beech Hill Road, Sheffield, UK

Graphical Abstract
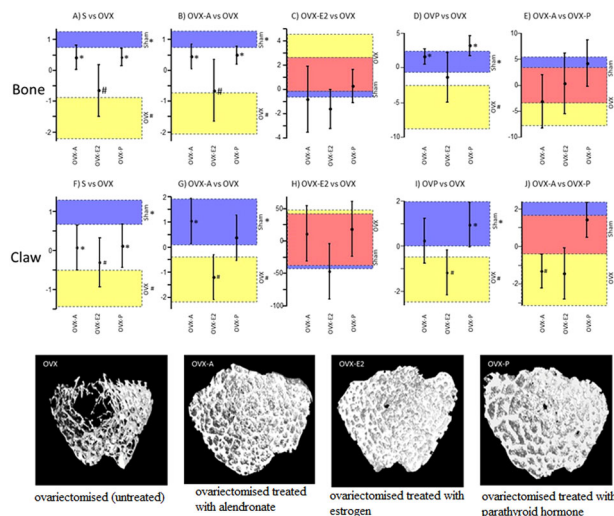
Highlights

- Osteoporotic treatments exhibit substantial differences in biochemical impact.
- Alendronate preserved the bone tissue in the state closest to the sham group.
- Parathyroid hormone prevents ovariectomy changes, induces different changes.
- Estrogen preserves tissue macro structure, but unable to prevent biochemical changes.
- Systemic conditions affect structural proteins in both bone and claw.

Abbreviations

ALN	alendronate
PTH	parathyroid hormone
E2	estrogen
OVX	ovariectomised (untreated)
OVXA	ovariectomised treated with alendronate
OVXE	ovariectomised treated with estrogen
OVXP	ovariectomised treated with parathyroid hormone
SEM	standard error of the mean
BMD	bone mineral density
DXA	Dual energy X-ray Absorptiometry
microCT	micro computed tomography
PCA	Principle Component Analysis
LDA	linear discriminant analysis
AUCROC	area under the curve for the receiver operator characteristics
ROI	region of interest

1 Introduction

Osteoporosis is a disease characterised by a reduction in bone mass, which can lead to bone fragility and increased susceptibility to fracture [1]. The disease affects both men and women, with incidence typically increasing with age [1]. Those most at risk from osteoporosis are post-menopausal women as the decline in estrogen (E2) level caused by the menopause triggers severe bone loss [1]. Measurement of change in bone mineral density (BMD) by Dual energy X-ray Absorptiometry (DXA) is the gold standard for clinical diagnosis of skeletal complications associated with osteoporosis. However, it is widely understood that the ability of bone to withstand physical stress and resist fracture depends not only on BMD but also other multiple factors including degree of mineralization, microdamage and the organization of collagen fibres mediated by the type and extent of collagen cross-links [2].

Raman spectroscopy is a sensitive and non-invasive optical technique that is commonly used in forensic and pharmaceutical studies, and it has been identified as a potential tool for evaluating bone protein using nail keratin as a surrogate marker [3–6]. The authors have previously shown that Raman spectroscopy is effective for predicting fracture risk based on assessment of nail keratin [7–9], and more recently reported that Raman spectroscopy predicted the link between claw keratin and bone collagen structure in a rodent model of osteoporosis [10]. Monitoring the response to anti-osteoporotic therapy is an important part of successful management of the disease in patients [11] and it has been acknowledged that changes to BMD may account for as little as 16% of the fracture risk reduction observed in bone active medication [12]. Encouraged by our recent findings, we hypothesise that Raman spectroscopic analysis of the fibrous proteins

collagen and keratin could be of value in monitoring the response to pharmacological therapy of osteoporosis and capture an aspect of therapeutic impact that is currently unevaluated.

The approved pharmaceutical agents for treatment and prevention of bone loss predominantly fall into two classes, anti-resorptive and bone anabolic. Bisphosphonates are a class of anti-resorptive drugs that bind to and accumulate in the bone mineral matrix with high affinity [13]. The anti-resorptive effect of Bisphosphonates is sustained even after treatment has stopped [13]. In 1995 alendronate (ALN) was the first bisphosphonate approved for the treatment of osteoporosis in the US. Clinical evaluation has shown ALN increases BMD [14] and reduces fracture risk in women [15–17]. Estrogen (E2) deficiency is an important contributing cause of osteoporosis, and thus E2 alone or hormone replacement therapy involving E2 and progestin is an effective therapy for osteoporosis [18]. Teriparatide, the human recombinant Parathyroid hormone (PTH) peptide 1−34, had been the only FDA approved anabolic agent [19] until an analogue of PTH-related protein (PTHrP) was recently approved by FDA for treatment of osteoporosis [20]. A number of clinical studies have shown that PTH treatment reduces fracture risk and increases BMD [21, 22], however further investigation of the long-term safety and efficacy ($\geq$ 2 years) is required [22]. Whilst both anabolic and anti-resorptive therapy for osteoporosis reduces bone fragility, encourages bone formation and reduces risk of fracture, these effects cannot be attributed only to the increase in bone mineral density (BMD).

In this study, we used an integrative approach that utilises data from Raman microscopic analysis of the fibrous proteins collagen and keratin, and microCT analysis of bone volume and architecture to assess the response of ovariectomised rats to E2 replacement, to anti-resorptive ALN and to bone anabolic PTH. Our results provide evidence to suggest that Raman Spectroscopy analysis of structural changes of fibrous proteins could be of value in monitoring the effects of the pharmacological treatments of osteoporosis.

2 Materials and methods

2.1 Animal experiments

All animal experiments were approved by the Animal Welfare and Ethical Review Body of the University of Edinburgh (Scotland, UK) and conducted in accordance with the UK Animals (Scientific Procedures) Act 1986. Animals were housed under standard conditions of temperature (25 ± 1 °C) and relative humidity ($60 \pm 10\%$) on 12 h light/dark cycle with *ad libitum* access to standard pellet diet and tap water.

Ovariectomy or sham ovariectomy was performed in 12 weeks old Sprague–Dawley rats as previously described [23]. The experiment was terminated on day 77 and bone mineral density was measured at the tibial metaphysis by micro computed tomography (microCT).

2.2 Animal study design

The animal study was designed and carried out at the University of Edinburgh (Scotland, UK).

A total of 56 Sprague–Dawley rats (23 weeks old at sacrifice) were used in this study as following ovariectomy they provide a suitable model of postmenopausal osteoporosis.

The rats were randomly assigned to 1 of 5 groups and underwent surgical intervention and treatment; the duration of intervention was 12 weeks (Table 1). Groups 1 and 2 are the same animals used in preparation of our recent study on the parallel impact of ovariectomy on both bone and claw tissues [10].

After completion of surgical intervention the bone samples (right femur) were collected and stored at −20 °C, and the claw samples (right and left claw) were collected and stored at 4 °C.

2.3 Sample analysis using Raman spectroscopy

The bone and claw samples were analysed using Raman spectroscopy at Queen's University Belfast (Belfast, UK) as previously described [10]. Briefly, Raman spectra were recorded using an Avalon Instrument RamanStation R1 (Avalon Instruments, Belfast, UK) at excitation wavelength 785 nm with a spectral resolution < 4 cm^{-1}. Exposure times of 18 and 15 s were recorded with a total of 196 and 45 spectra collected in a grid on each bone and claw sample, respectively. The analyst was blinded to sample treatments

Table 1 Study design, surgery and treatments

Group	Surgical intervention	Treatment	N
Sham	Sham OVX	Vehicle (dH$_2$O)	11
OVX	OVX	Vehicle (dH$_2$O)	11
OVX-A	OVX	Alendronate (1 mg/Kg per week)	11
OVX-E2	OVX	Estrogen (75 μg/Kg, once during surgery)	11
OVX-P	OVX	Parathyroid Hormone (75 μg/Kg, 3 per week)	12

OVX Ovariectomy, *OVX-A* ALN, *OVX-E2* E2, *OVX-P* PTH, *N* number of rats per group, *dH$_2$O* distilled water

throughout data acquisition and data processing. Sample stability was tested by exposing the samples under the same conditions for 10x longer than the planned analytical time followed by PLS regression against time and no changes were observed.

2.4 Data analysis of Raman spectroscopy spectra

Spectral processing was as previously described [10] with cosmic rays manually removed, baseline correction [24, 25] and principle component analysis (PCA) based normalisation [26, 27]. Data reduction of the normalised data was performed using PCA followed by a *t*-test to check of significant differences between groups. The resulting reduced data set was used to calculate a linear discriminant analysis (LDA) whose scores were used to calculate sensitivity, specificity and area under the curve for the receiver operator characteristics (AUCROC) performance characteristics. To evaluate the impact of the pharmaceutical agents on the bone and claw tissues compared to OVX, LDA models were applied to the spectral data including OVX against OVX-A (1st PC), OVX-E2 (9th PC) and OVX-P (1st, 2nd and 8th PC).

Partial subtraction bone and claw spectra for detailed evaluation were calculated by scaling the subtrahend to the point just before any negative features appeared in the result.

Based on published methods [28, 29], the intensities of three chemical constituents of bone were calculated as:

1. Apatite—mean intensity from 948–978 cm^{-1} minus the mean local baseline at 896–904 and 988–996 cm^{-1}
2. Protein—mean intensity from 1100–1300 cm^{-1} and since no individual peak was to be discriminated no local baseline was calculated
3. Carbonate (type B substitution)—mean intensity from 1062–82 minus the mean local baseline at 1052–1056 and 1092–1096 cm^{-1}.

The ratio of apatite intensity to protein and to carbonate were calculated for each sample before calculating the mean ratio and its standard deviation and 95% confidence intervals within each treatment group. Unpaired *T*-tests were used to compare the ratios between groups.

The percent protective effect of treatments was analysed as the proportion of a parameter change upon treatment relative to that of the change observed between sham and ovariectomised. This was calculated as

$$\text{Percent Protective Effect} = 100 - 100 * \frac{S - T}{S - O}$$

Where S is the parameter value in the sham group, T is the parameter value in the treatment group and O is the value in the ovariectomised group. Briefly this value would be expected to be 100 if T is identical to S (T is completely protective), 0 is it fails to modulate the OVX induced change. Values above 100 indicate that a change is induced in the opposite direction to the OVX, while a value below 0 would indicate an enhancement of the OVX induced changes.

2.5 Micro-computed tomography

Bone architecture was assessed using microCT at the University of Edinburgh (Scotland, UK). Trabecular and cortical bone parameters were analysed as previously describe by Campbell & Sophocleous [30], using a Skyscan 1172 instrument (Brucker, Belgium) set at 70 kV and 142μA and at a resolution of 10 μm. Acquired images were then reconstructed using the Skyscan NRecon program and analyzed using Skyscan CTAn software (Bruker Micro-CT). Trabecular bone was analysed at the left distal femoral metaphysis, on a region of interest (ROI) extending 1 mm proximally from the proximal tip of the primary spongiosa. Analysis of cortical bone focused on a region extending 1.25 mm distally from the midpoint of the femur. The ROI was selected adjacent to the endocortical surface using a freehand drawing tool at five to seven different levels. Auto-interpolation between these levels produced the total ROI for all frames selected.

2.6 Statistical analysis

Significant differences between groups with regard to % change from vehicle-treated sham-operated rats (sham-veh) were assessed using one-way analysis of variance (ANOVA) followed by Tukey HSD post hoc test (for equal variances) or Games– Howell post hoc test (for unequal variances). The significance threshold level was set at $p < 0.05$.

2.7 Scatter graphs

For plotting the parameter changes they were standardised against the value observed in the sham. For values with an absolute scale these were calculated as the percentage change from the sham vehicle:

$$\text{percentage change from the sham vehicle} = 100 * \frac{T - \bar{S}}{\bar{S}}$$

For discriminant scores (which measure the relative balance of two extreme factors) the scores were standardised to unit sham value:

$$\text{standardised discriminant score} = \frac{T}{\bar{S}}$$

The data was plotted with shaded blocks representing the confidence intervals for parameter values of sham (blue, RGB [0,0,0.5]) and OVX (yellow, RGB [0.5,0.5,0]) as the background variation that we wish to compare our treatments against. Overlap of these boxes is coloured red (RGB [1,0.5,0.5]), which indicates overlap of the 95% confidence intervals. Mean of each treatment group is plotted over these blocks along with error bars representing the 95% confidence interval.

3 Results

3.1 ALN, E2 and PTH protect against ovariectomy-induced bone loss in rats

MicroCT analysis of bone at the tibial metaphysis confirmed that administration of ALN (OVX-A), E2 (OVX-E2) and PTH (OVX-P) in rats protected against ovariectomy-induced bone loss as evident by increased trabecular bone volume (BV/TV) (Fig. 1a). In addition the treatments all maintained trabecular separation (Tb.Sp) and pattern factor (Tb.Pf) and trabecular number (Tb.N) closer to that found in the sham group than the ovariectomised group (Fig. 1b, c and e, Table 2).

Analysis of the cortical compartment of bone showed that ALN and PTH induced gain in cortical bone volume while E2 fell somewhere between the values of sham and OVX (Fig. 1f). The same treatments induced increases in cortical thickness (this had been unaffected by ovariectomy). Ovariectomised rats that received PTH treatment (OVX-P) exhibited a dramatic increase in the thickness of both trabeculae and cortex (Fig. 1d, g) when compared to ALN (OVX-A) or E2 (OVX-E2), indicative of the bone anabolic activity of PTH. Note that there was no significant difference in either thickness between the sham and ovariectomised, indicating this is a change that is independent of effects that can be attributed to the ovariectomy procedure.

3.2 E2, but not ALN or PTH, counteracted ovariectomy-induced body weight gain in rats

E2 deficiency caused a significant gain in body weight in ovariectomised rats and this was significantly prevented by E2 (OVX-E2) (Fig. 1h). In contrast, ALN (OVX-A) and PTH (OVX-P) treatments had no significant protective effect on ovariectomy-induced body weight gain (Fig. 1h).

3.3 Bone and claw Raman signatures

Figure 2a i, iii illustrate the Raman signatures of rat bone and claw tissue as compared to spectra recorded from purified samples of hydroxyapatite, collagen and keratin (Figure 2a ii, iv, v, respectively). Literature based assignments for the major peaks present in the spectra are provided in Table 3. Raman spectroscopy reveals characteristic vibrational frequencies within the both the mineral and collagen matrix phases of the bone, and within claw keratin. The peaks that dominate the bone spectrum below $1100 \, \text{cm}^{-1}$ are attributable to primarily mineral components of the bone, while the main contributor to the peaks above $1100 \, \text{cm}^{-1}$ is collagen matrix. Comparison between the protein region of the bone (collagen) and the same region of the claw keratin spectrum shows similar protein peaks are present in both tissues, including amide III, CH_2 and amide I.

3.4 Evaluation of how osteoporosis pharmaceutical agents alter bone and tissue structure using Raman spectroscopy

As shown previously, ovariectomy alters the secondary and tertiary structures of bone and claw tissue in a similar and concurrent manner [10], with ovariectomy inducing a less ordered structure within both collagen and claw keratin. In this study, using the same animal model as previously, the impact of ovariectomy (OVX) followed by treatment with ALN, E2 or PTH on bone and claw tissue structure compared to the OVX without treatment groups and also to sham operation animals was evaluated by detailed analysis of Raman spectra. The partial subtraction mean Raman spectra for bone (Fig. 2b) and claw (Fig. 2c) for (i) OVX-A, (ii) OVX-E2, (iii) OVX-P minus the OVX are shown.

The bone spectral signatures show OVX-A appears more similar to OVX-P than any other group, while OVX-E2 visually appears very similar to the OVX spectrum. The protein peaks are relatively weak in both the OVX-A and OVX-P spectra, indicating demineralisation was reduced by these two treatments, while more has occurred in the OVX-E2 group. This visual interpretation is strengthened by statistical analysis of the ratio of mineral to protein features in the respective spectra (Table 4). The variation in apatite to protein ratio, derived from the Raman features, is shown in Fig. 3a. None of the interventions were capable of maintaining the mineral to protein ratio present in the sham, but ALN and PTH were able to significantly reduce the impact of the ovariectomy by a factor of 0.45, reducing loss from 16 (13.8–18.6) to 7.5 (5.5–9.6) % of the sham mean. The trend for apatite to carbonate ratio is shown in Fig. 3b, where it is observed that ALN maintained the level of carbonate substitution equivalent to that of the sham, while E2 failed to significantly prevent alteration to levels observed in the untreated ovariectomised rats (ratio of apatite to carbonate declined by 2.3 (1.7–2.9) %. PTH increased the ratio of apatite to carbonate by 2.7 (2.0–3.4) % relative to the mean value observed in the sham group.
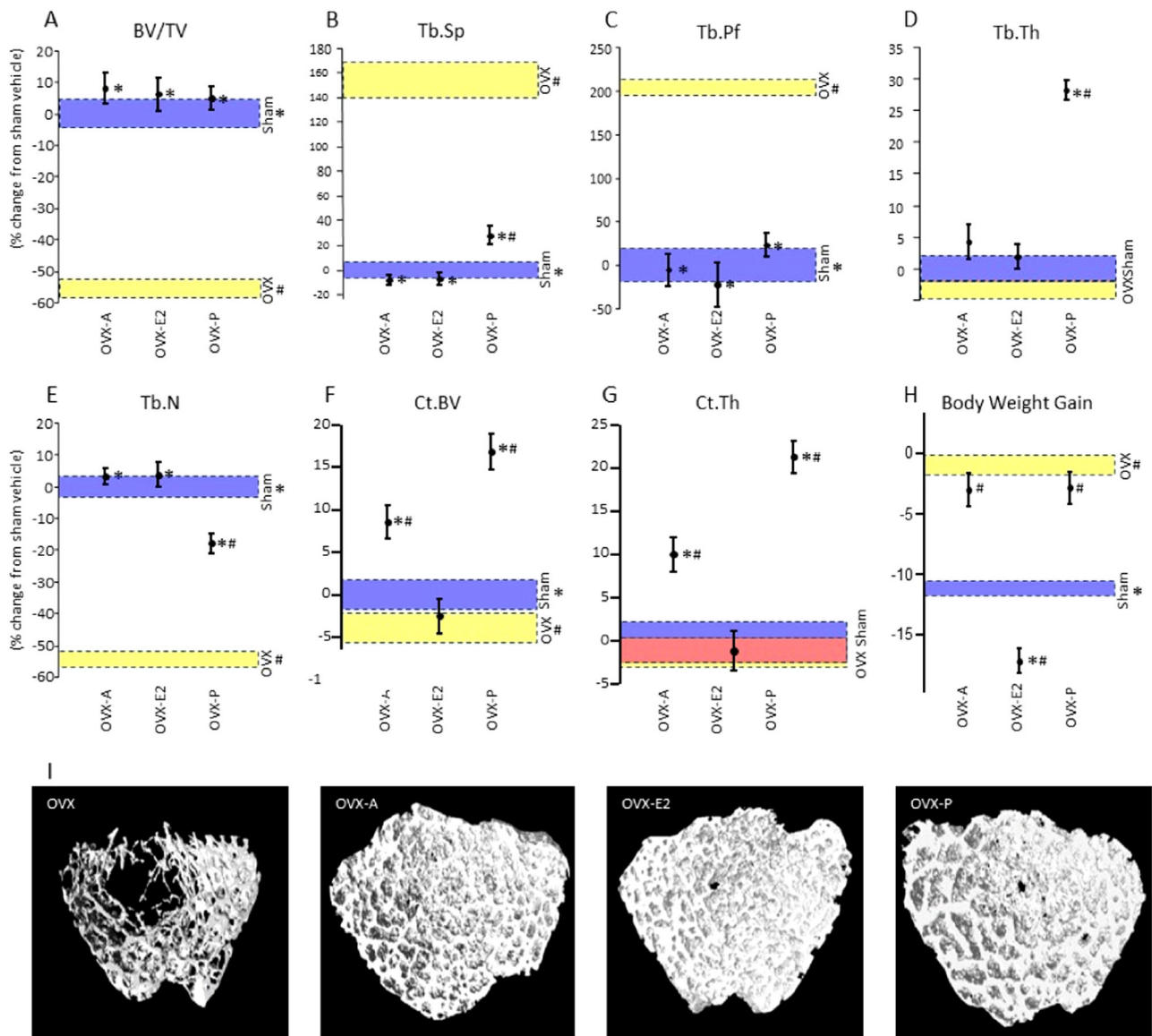
Fig. 1 (A:G,I) % change from sham group for parameters derived from MicroCT analysis of bone at the distal femoral metaphysis and diaphysis of ovariectomised rat treated with vehicle (OVX), ALN (OVX-A), E2 (OVX-E2) or PTH (OVX-P) and sham operation rats (sham). **a** Trabecular bone volume (BV/TV); **b** Trabecular Separation (Tb.Sp); **c** Trabecular pattern factor (Tb.Pf); **d** Trabecular thickness (Tb.Th); **e** Trabecular Number (Tb.N); **f** Cortical bone volume (Ct.BV); **g** Cortical thickness (Ct.Th); **h** Body weight gain; **i** Representative images of microCT analysis. Values are means ± SEM from 10–12 mice. #$p < 0.05$ from sham; *$p < 0.05$ from OVX. Blue and yellow regions are non-overlapping regions of the 95% confidence intervals for sham and OVX groups, respectively, while the red region indicates overlap

3.5 Discrimination between OVX and drug treatments using a LDA models

Previously, we have shown that healthy bone and claw tissue can be discriminated from osteoporotic tissue using a LDA model calculated based on Raman spectral data [10]. Here we have used the same model to test whether bone and claw tissue from animals that underwent ovariectomy followed by treatment with either ALN, E2 or PTH can be discriminated from baseline, sham OVX, OVX or the different treatments administrated.

Figure 4 shows the Sprague-Dawley bone sample LDA results for a range of models projected onto each group, with p-values for the sham-OVX model projected onto the others listed in Table 5. This shows how the variation separating any two groups is shared with the remaining groups in the data set. The LDA based on the changes between sham and ovariectomised classified the sham group and OVX-A and OVX-P groups as significantly different to OVX, whereas OVX-E2 was not significantly different to the OVX (Table 5). When comparing OVX to the other treatments (Table 5), all were significantly

Table 2 Stastical analysis showing *p*-values for unpaired *t*-tests between treatments for the microCT parameters listed in each section header and body weight gain

BV/TV (%)

	Ovx	Ovx-A	OVX-E2	Ovx-P
Sham	4×10^{-8}	0.263	0.611	0.441
Ovx		7×10^{-9}	2×10^{-7}	6×10^{-11}
Ovx-A			0.583	0.608
OVX-E2				0.447

Tb.Th (U)

	Ovx	Ovx-A	OVX-E2	Ovx-P
Sham	0.198	0.220	0.514	4×10^{-10}
Ovx		**0.027**	0.061	3×10^{-12}
Ovx-A			0.496	2×10^{-7}
OVX-E2				1×10^{-9}

Tb.Sp (U)

	Ovx	**Ovx-A**	**OVX-E2**	**Ovx-P**
Sham	5×10^{-7}	0.188	0.512	**0.008**
Ovx		5×10^{-7}	4×10^{-7}	2×10^{-6}
Ovx-A			0.534	3×10^{-4}
OVX-E2				**0.006**

Tb.N (1/U)

	Ovx	**Ovx-A**	**OVX-E2**	**Ovx-P**
Sham	4×10^{-10}	0.462	0.766	**0.001**
Ovx		3×10^{-12}	5×10^{-10}	3×10^{-8}
Ovx-A			0.705	4×10^{-5}
OVX-E2				**0.001**

Body weight gain

	Ovx	**Ovx-A**	**OVX-E2**	**Ovx-P**
Sham	4×10^{-8}	5×10^{-5}	6×10^{-5}	6×10^{-5}
Ovx		0.26	8×10^{-10}	0.26
Ovx-A			3×10^{-8}	0.99
OVX-E2				2×10^{-8}

Values below 0.05 are bolded to indicate statistically significant results

different with OVX plus E2 having the smallest effect size.

Comparing OVX to the other treatments, OVX is significantly different from the sham OVX. None of the OVX plus treatment (ALN, E2 and PTH) groups were significantly different from OVX alone, with the ALN treatment having the least impact.

However, the LDA results modelled on OVX against OVX-A (Fig. 4 for bone and claw, respectively) or OVX-P (Fig. 4c and F for bone and claw, respectively) show OVX-A is significantly different from OVX alone in both models. The

PTH treatment group is also significantly different from OVX group in the OVX against OVX-P models (both tissues) and the OVX-A bone model. In the latter models, OVX-E2 is classified as more similar to OVX. When the OVX against OVX-E2 model was applied (Fig. 4b), the E2 treatment was classed as significantly different from OVX; however, this model had a lower AUCROC value of 76%, while the claw model was not significant with an AUCROC of 55%.

In Fig. 5 i, ii the difference between the treatment vs sham discriminant function and the ovariectomy vs sham discriminant function is shown. This subtraction operation removes the variation that can be explained as a direct prevention of the expected effects of an ovariectomy. This leaves the residual signal as the variation induced by the treatment that is not related to prevention of ovariectomy induces changes. In both the claw and the bone the ALN exhibits lower residual variation than PTH, suggesting that the ALN is maintaining the bone collagen and the claw keratin in a state closer to the expected physiological state of the sham group.

3.6 Differences between drug treatments

Figure 4 allows observation how the pattern of the variation described by each model varies within each treatment. The sham vs OVX and ALN vs OVX show very similar patterns across all models, while E2 shows weak effects in all these models. This is echoed in the PCs used by each model, with the sham-OVX (PC 1,5), OVX-OVXA (PC 1) and OVX-OVXP (PC 1,6,8) models share contribution from the 1st PC, suggesting a common factor in the associated variation. The OVX-OVXE only uses PC9, which is not exploited by any other model suggesting its variation is orthogonal to the effect of ovariectomy and a mechanism of response that is orthogonal to the other two treatments. Furthermore, the OVX-OVXE model uses the lowest ranked PC of any other study, indicating the weakest effect. Compared to the sham the OVX is consistently lower, with the biggest difference occurring for the PTH vs OVX model. Models involving PTH are only models to give scores exceeding the sham, with the largest differences occurring in the PTH samples themselves.

Figure 5 i, ii show an expanded view of the amide I and III regions of the discriminant functions created when classifying each pair of treatments in the bone and the claw tissues after correction against the sham-OVX model. A treatment that perfectly preserves the physiology of the sham group would therefore exhibit only noise in the residual, while any deviations from that physiological state will be evident in the subtraction. It is noticeable that in both tissues the peak at $1656 \, \text{cm}^{-1}$ follows the same trend, with negative peaks with intensity ranked E2 > PTH > ALN. This was a key change observed in the progression of the ovariectomised rats, reflecting a disordering in the proteins with
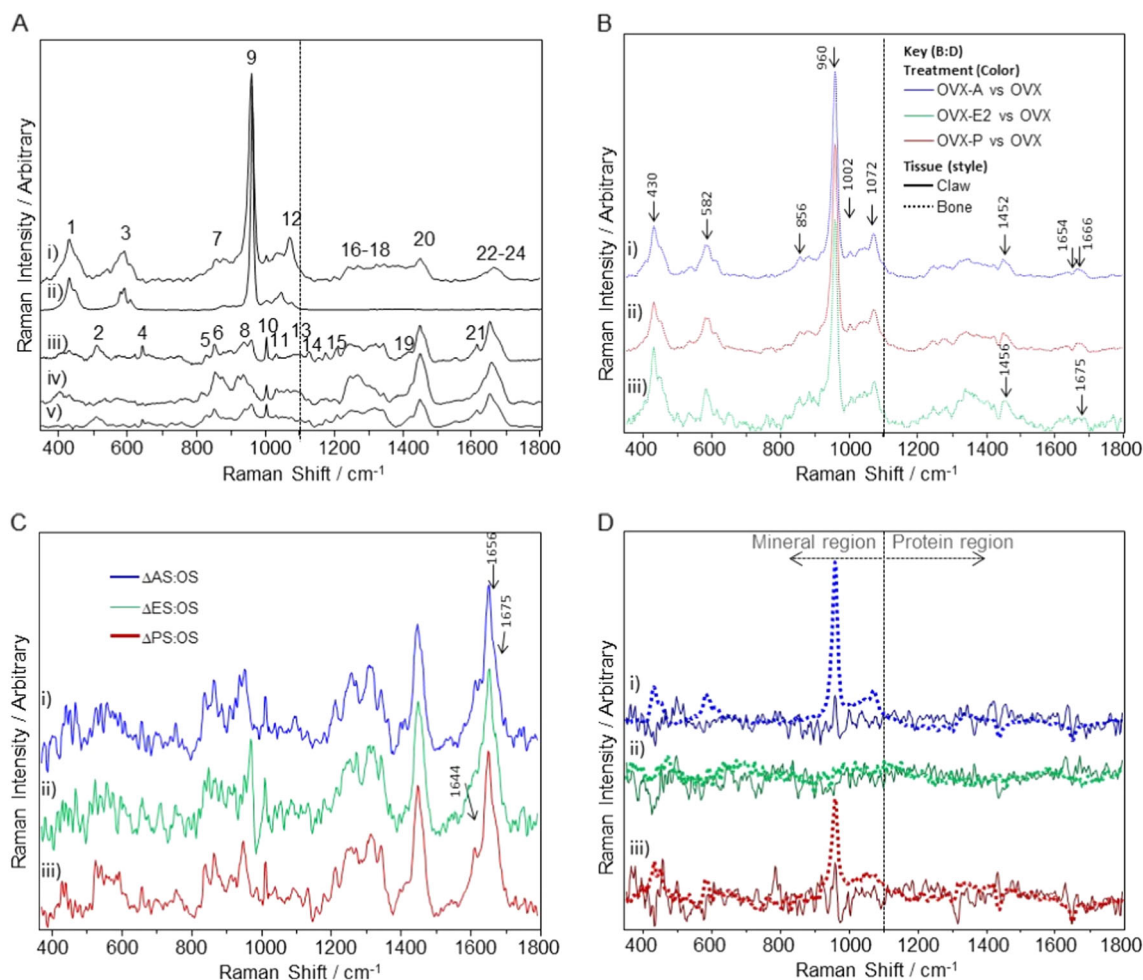
Fig. 2 Effect of treatments after ovariectomy on the Raman spectroscopic signatures of bone and claw tissues. **a** Average normalised Raman spectra of Sprague-Dawley bone (i) and claw (iii) samples. The average spectra for the bone and claw models are compared to hydroxyapatite (ii), collagen (iv) and keratin (v). **b**, **c** Subtraction spectra for average (i) OVX-A, (ii) OVX-E2 and (iii) OVX-P minus OVX from bone **b** and claw **c** samples. Selected Raman bands are labelled against Table 3 with the corresponding wavelength in brackets. **d** The discriminant function for Sprague-Dawley (i) OVX-A, (ii) OVX-E2 and (iii) OVX-P vs OVX models, with dashed line for bone and solid line for claw samples

the development of pathology. In addition, the peak corresponding to b-sheet conformation shows the same trend, with a shift in peak centre from 1672 for PTH to 1678 cm^{-1} for E2 within bone (shift not observed in the claw tissue). Globular alpha helices, identified by peaks at 1645 and 1305 cm^{-1} were more prevalent in the bone with PTH and ALN treatments, with E2 exhibiting the lowest rate of globular alpha helix formation. In the claw tissue exhibits a much stronger response in terms of globular alpha helix.

The spectra also suggest the level of ionisation of amino acid side groups between treatments, as evidenced by the peak around 1420 cm^{-1} for all three treatments. The peak at 1440 cm^{-1}, sensitive to how hydrophilic the local environment of the protein chain is. In all three treatments the peak at 1440 cm^{-1} is negative, indicating increased hydrophobic interactions compared with sham.

3.7 Protective effect

The percentage of change observed between the sham and ovariectomised groups was reduced for the key Raman derived parameters measured in this study (Table 6), with ALN and PTH exhibiting similar levels of protections and E2 exhibiting a weaker influence. ALN and PTH but only 35% for E2. Interestingly the changes in mineral content are unable to explain most of this reduction (a reduction of only 54% for ALN and PTH, 5% for E2), but the discriminant score calculated using the protein only region of the spectrum exhibits a much stronger preventative effect (80% for ALN and PTH, 26% for E2). The claw shows similar performance for ALN and PTH (53 and 56%, respectively) with E2 exhibiting a weaker protective effect (34%).

Table 3 Bone and claw Raman spectroscopy band assignments

Peak no.	Raman shift (cm^{-1})	Assignment	Keratin/Collagen/ Mineral	References
1	430	$PO_4^{3-} \nu_{2\,AS}$	Mineral	[44]
2	510	Disulfide, ν (S-S)	Keratin	[4]
3	580–590	$PO_4^{3-} \nu_{4\,AS}$	Mineral	[44]
4	644	Cysteine, ν (CS)	Keratin	[5]
5	830	Tyrosine, δ (CCH) $_{OP}$	Collagen/Keratin	[45]
6	850	Tyrosine/O-P-O, δ (CCH) ring breathing	Collagen/Keratin/ Mineral	[45]
7	856	Hydroxyproline	Collagen	[44]
8	936	α-helix, ν (CC)	Collagen/Keratin	[45]
9	960	$PO_4^{3-} \nu_1$	Mineral	[44]
10	1004	Phenylalanine	Collagen/Keratin	[45]
11	1032	Phenylalanine	Collagen/Keratin	[45]
12	1070	CO_4^{3-} (ν)	Mineral	[46]
13	1078	Carbon backbone, ν (CC) $_{RC}$	Collagen/Keratin	[45]
14	1126	Carbon backbone, ν (CC) $_{TC}$	Collagen/Keratin	[45]
15	1206	Tyrosine and Phenylalanine, ν (C-C$_6$H$_5$)	Collagen/Keratin	[45]
16	1240	β-sheet, Amide III	Collagen/Keratin	[44]
17	1256	Random, Amide III	Collagen/Keratin	[45]
18	1305	α-helix, Amide III	Collagen/Keratin	[44]
19	1420	C-H bonding, δ (CH$_3$) deformation	Collagen/Keratin	[45]
20	1450	C-H bonding, δ (CH$_2$) scissoring	Collagen/Keratin	[45]
21	1614	Tyrosine and Tryptophan, C = C stretching	Keratin	[45]
22	1642–44	α-helix, ν (CO) amide I	Collagen/Keratin	[47]
23	1652–56	Random, ν (CO) amide I	Collagen/Keratin	[47]
24	1668–75	β-sheet, ν (CO) amide I	Collagen/Keratin	

The main peaks present in the bone and claw spectra are listed in numerical order including their wavenumbers, band assignments, whether they are keratin, collagen or mineral bands and band assignment references. Asymmetric stretch (AS), out of plane (γ), in plane (δ) random conformation (RC), trans conformation (TC) and stretch (ν)

AS asymmetric stretch, γ out of plane, δ in plane, RC random conformation, TC trans conformation, ν stretch

Table 4 P-values from unpaired t-test for the ratio of apatite to protein peaks in the Raman spectra of bone from each experimental group

	Ovx	Ovx-A	OVX-E2	Ovx-P
Apatite/Protein				
Sham	**2.8e-05**	**0.011**	**0.003**	**0.004**
Ovx		**0.013**	0.877	**0.006**
Ovx-A			0.098	0.984
OVX-E2				0.074
Apatite/Carbonate				
Sham	**0.036**	0.793	0.0846	**0.026**
Ovx		**0.007**	0.650	**2.65e^{-5}**
Ovx-A			**0.024**	**0.023**
OVX-E2				**0.0001**

Values below 0.05 are highlighted in bold

4 Discussion

The clinical application of ALN, E2 or PTH in the treatment of osteoporosis enhances BMD and reduces risk of fracture in in postmenopausal women [31–33]. However, the osteoprotective and bone anabolic effects associated with these treatments cannot be attributed only to the increase in BMD [34]. Bone quality and fragility also depend on the maturation, orientation and organization of fibrous proteins [35, 36]. We have recently used a rodent model of osteoporosis to show that analysis of keratinous tissue by Raman spectroscopy acts as surrogate marker for monitoring bone health deterioration caused by E2 deficiency in rats [10]. In this study, we assessed the effects of post-ovariectomy administration of ALN, E2 or PTH on structural changes

Fig. 3 % change from sham group for mineral parameters derived from the Raman spectra **a** apatite band to protein band intensity ratio **b** Phosphate to Carbonate ratio
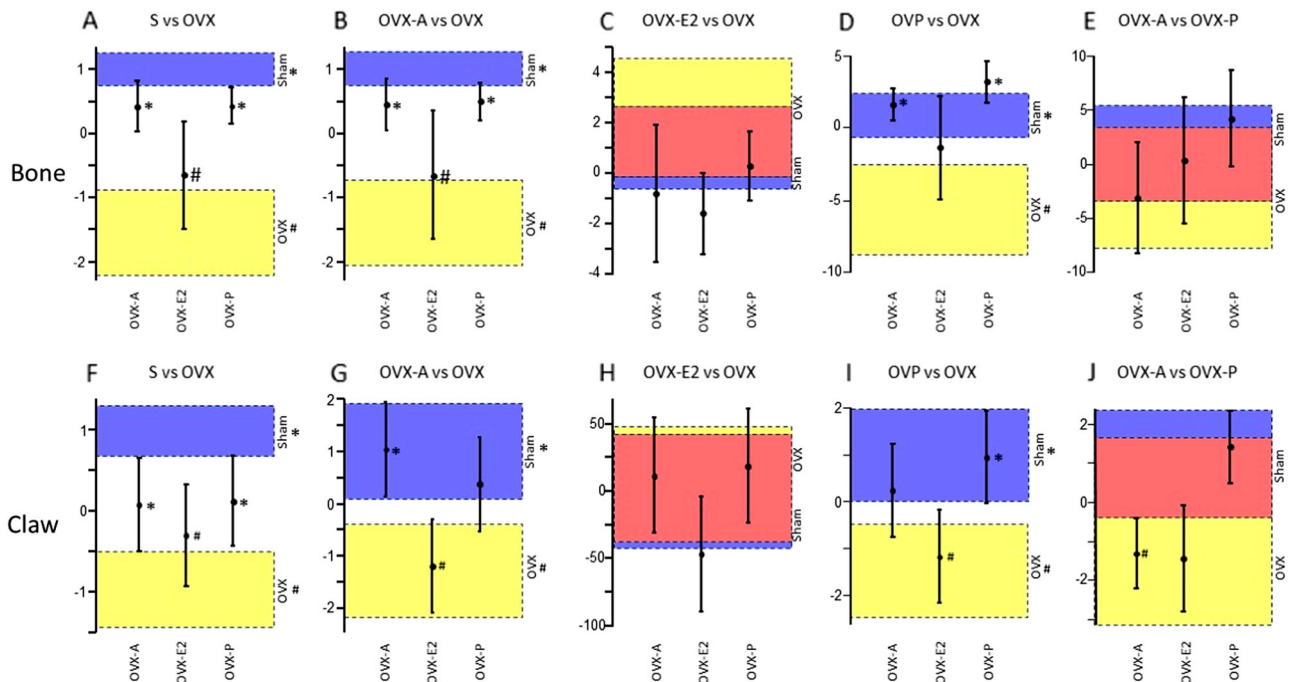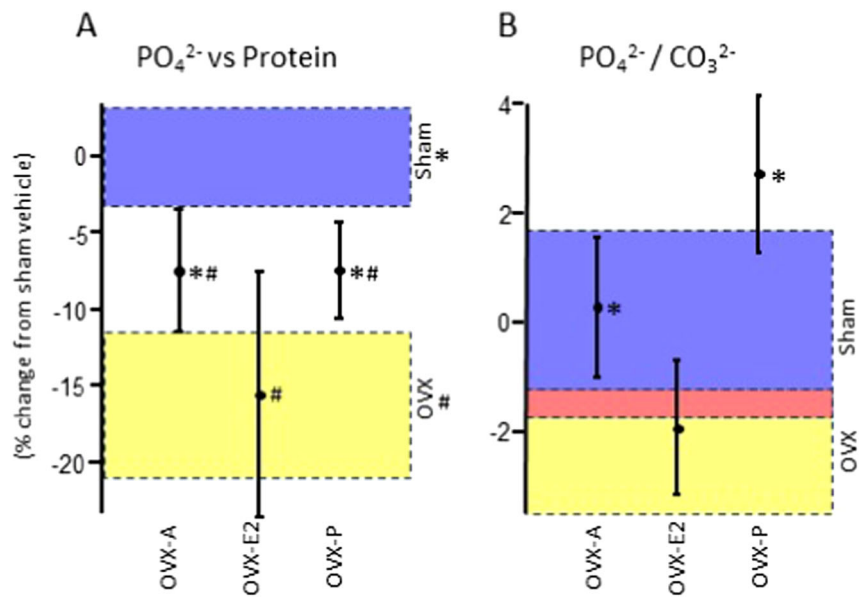

Fig. 4 Comparison of the discriminant scores by treatment for a range of discriminant models derived from Raman measurement of bone **a**–**e** and claw **f**–**j** tissue. Models were created to discriminate between the specified groups then projected onto all samples. Scores were normalized against the mean for the sham group within each model. The models are **a**, **f** sham vs OVX, **b**, **g** OVX-A vs OVX, **c**, **h** OVX-E2 vs OVX **d**, **l** OVX-P vs OVX and **e**, **j** OVX-A vs OVX-P. Values are means ± SEM from 10–12 mice. #$p < 0.05$ from sham; *$p < 0.05$ from OVX. Blue and yellow regions are non-overlapping regions of the 95% confidence intervals for sham and OVX groups, respectively, while the red region indicates overlap

within the bone tissue (collagen and mineral phases), and claw tissue (keratin) using Raman spectroscopy. Our data provide evidence to suggest that Raman spectroscopy can act as predictive tool for monitoring pharmacological therapy of osteoporosis in rodents.

4.1 Analysis of effects of anti-osteoporotic treatments on long bones

Although ALN, E2 and PTH have been used for many years to treat and prevent osteoporosis and their influence on

Table 5 *p*-values for *T*-test between OVX-Sham discriminant scores for pairs of treatments within the bone and claw tissue

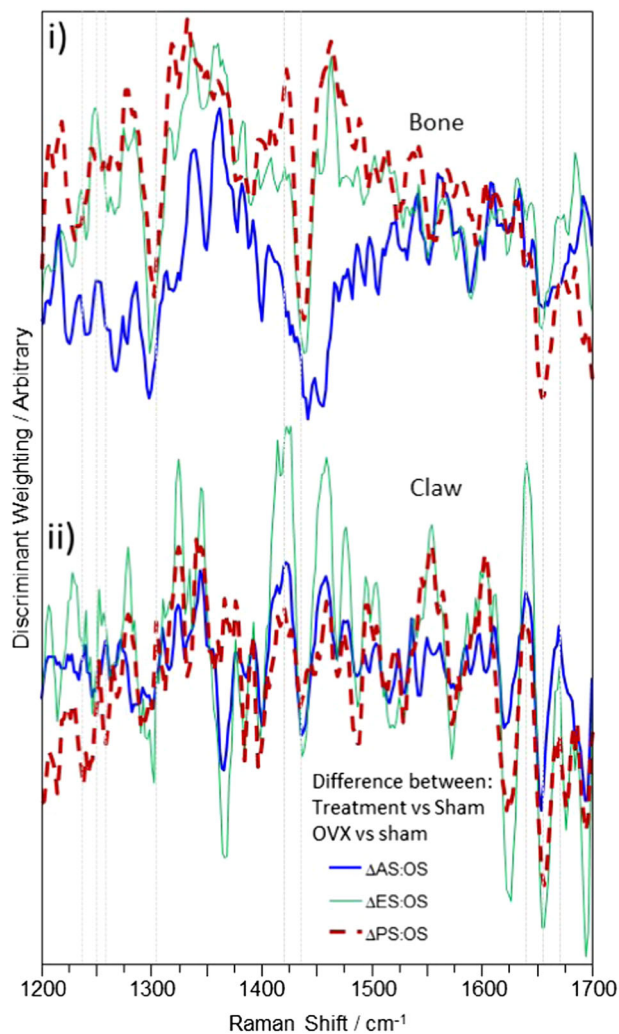|	Ovx	Ovx-A	OVX-E2	Ovx-P
Bone				
Sham	**5.37e^{-6}**	**0.044**	**0.008**	**0.022**
Ovx		**0.0002**	0.239	**3.62e^{-5}**
Ovx-A			0.067	0.814
OVX-E2				**0.037**
Claw				
Sham	**2.93e^{-6}**	**0.016**	**0.002**	**0.035**
Ovx	0	**0.0101**	0.119	**0.009**
Ovx-A	0	0	0.342	0.878
OVX-E2	0	0	0	0.285

Values below 0.05 are highlighted in bold

Fig. 5 Protein only region of the difference between discriminant models for treatment vs OVX minus sham vs OVX. These models were derived based on Raman spectroscopic measurement of (i) bone tissue and (ii) claw tissue. Vertical lines indicate peaks discussed in the text

BMD has been well studied [31], how these agents effect bone collagen matrix and subsequently bone fragility is less well understood. The stability and maturity of collagen mediated through cross-link formation (intra- and inter-molecular) is understood to have significant importance (positive or negative) for bone toughness and post-yield bone properties [37]. Moreover, the disorder osteogenesis imperfecta is characterised by disorganized collagen and increased susceptibility to bone fracture. Thus, understanding how these osteoporosis agents impact on bone collagen is likely to be important in the reduction and prevention of bone fractures.

The microCT analysis of bones in our study indicates that all interventions tested prevented loss of bone material caused by ovariectomy in rats, with ALN and E2 offering similar macroscopic bone structure protection, while the PTH caused a similar effects but additionally it enhanced trabeculae thickness indicative of its anabolic activity. Analysis of microCT data is insufficient to detect the biochemical changes caused by E2 deficiency within the remodelled rat tissue. In contrast, the Raman microscopic signature indicates that a number of critical changes to bone composition do occur, indicating that reliance on gross anatomical information gives an incomplete picture.

The Raman data demonstrates that ALN and PTH are only able to prevent approximately half of the demineralisation that otherwise occurs in untreated ovariectomised rats, while E2 is not able to prevent any relative demineralisation. ALN is the only treatment that maintained physiological levels of carbonate relative to apatite, while E2 failed to prevent relative apatite loss and PTH encouraged a higher level of apatite relative to carbonate.

These results indicate that treatment with these agents prevents demineralization and modulates carbonate content. Furthermore, the Raman data suggests that E2 replacement failed to reverse the ovariectomy-induced changes in the mineral to protein ratio when compared to the sham group —unlike its effects on body weight gain and bone volume. These data suggest that while microCT analysis of bone reveals the effects of anti-osteoporotic treatments on the physical bone macro-structure in ovariectomised rats, the changes in biochemical composition are better detected by Raman microscopy.

ALN and PTH significantly protected the structure of bone collagen, with some overlap compared to sham and some subtle differences more prevalent in the PTH. E2 appears to be the most different, exhibiting very little reversal of biochemical composition of bone, as shown by which shows that the Ovx vs E difference is in a different direction to the difference between Ovx and Sham (as evidenced by the sham lying the same side of the zero line as the ovariectomised tissue) and for the OVX vs Sham model where the E2 shows only an insignificant amount of

Table 6 Percent protective effect achieved by each treatment for parameters affected by ovariectomy

	Overall bone discriminant score	Bone apatite to protein ratio	Bone protein discriminant score	Claw discriminant score
OVX-A	76.7	53.8	80.2	53.2
OVX-E	34.5	4.6	26.2	33.7
OVX-P	77.2	54.1	78.2	55.7

reversion to the ovariectomy-induced changes. ALN and PTH prevented some ovariectomy-induced changes in bone but each treatment also caused some changes not related to ovariectomy with ALN showing the smallest additional changes. This is particularly interesting in the light of the clear difference in morphological features (esp. trabecular thickness ad spacing) that was observed after PTH administration. These general observations agree with where the subtraction spectra for OVX-A and OVX-P are visually similar, while the OVX-E2 subtraction exhibits a different spectral profile.

ALN treatment (10 mg/day) for three years has been shown to reduce fracture rate by increasing bone strength facilitated through a higher degree of mineralization [38] and crystalline homogeneity [38, 39]. The impact of ALN on collagen structure has also been assessed by Allen et al. [35, 40]. Using a skeletally mature canine model they demonstrated ALN can alter collagen cross-linking (enzymatic (pyridinoline (PYD) and deoxypyridinoline (DPD)) and non-enzymatic (pentosidine (PEN)) and increase collagen isomerization (decreased α/β C-telopeptide (CTX) ratio compared to vehicle), and the authors suggested these changes may impact on bone fracture risk [35, 40]. Their results also indicate that ALN lowered the rate of bone remodelling and this effect was adversely correlated with increased non-enzymatic cross-links that are associated with enhanced microdamage [40]. This adverse effect of ALN treatment has also been observed in data from a skeletally mature canine model treated with high doses of the bisphosphonate [41], in which the authors concluded that these effects may impact fracture resistance [41]. A major limitation of these studies is that the models used were healthy [35, 40], and as such the reported effects of bisphosphonate treatment may not apply to osteoporosis. Contrasting with these studies, the data presented in the present study suggest that ALN alter collagen structure post-ovariectomy as evident by the ALN Raman microscopic signature that is different to those observed in sham and ovariectomised rats, although much closer to sham group than to the ovariectomised group.

The results of the present study have shown that administration of E2 treatment post-ovariectomy in rats—unlike ALN and PTH interventions—shows a similar Raman profile to ovariectomy alone. Thus, suggesting that the hormone treatment of E2 has minimal protective

capability for the bone composition and the organisation of the mineral or matrix phases. Paschalis et al. have shown that E2 hormone treatment modifies collagen structure; following 2 years of hormone replacement therapy (HRT) there was an increase in collagen cross-links ratio by 40% in iliac crest biopsies taken from postmenopausal women measured using Fourier transform infrared microscopic imaging [42]. While the findings from Paschalis were based on a different treatment regime (cyclic E2 and progestogen), treatment duration and model as well as measurement technique used, such a mechanism may explain why the protein phase does not show a reversion of ovariectomy-induced changes. The LDA bone model findings indicate the ovariectomized and ovariectomized plus E2 groups are significantly different, albeit having the least significance of the treatment groups. The results indicate that the majority of the protective effects against OVX are common between ALN and PTH but there are differences between the two (Figs. 3a, 4 and 5). The ALN shows very similar pattern of scores compared to sham under all the LDA models presented, suggesting that the majority of its influence is prevention of changes that would otherwise be induced by the ovariectomy, although the quantity is not quite fully reversed.

Saito et al. have shown that PTH treatment altered collagen cross-links; increased enzymatic cross-links and, dissimilar to ALN treatment, decreased non-enzymatic cross-links suggesting a reduction in collagen maturation, and suggested these alterations improved bone strength [36]. A study measuring biopsies from osteoporotic postmenopausal women using confocal and electron microscopy has also shown PTH (1–34) treatment significantly altered the orientation of collagen fibres compared to pretreatment. Moreover, they showed PTH treatment increased mineral calcification using micro-X-ray data [43]. In the present study, the models including PTH explicitly (PTH vs OVX and ALN vs PTH) show that the PTH exhibits another qualitative change that is much more strongly evident in this treatment group than any other. Unlike the maintenance associated with ALN, the PTH appears to induce new changes in the bone tissue not observed in the sham nor ovariectomised groups, suggesting that this treatment is introducing new elements to the bone structure or composition. Both ALN and PTH indicate a protection of the bone mineral to protein ratio upon treatment. In contrast the E2

Raman data suggests that this treatment has a much lower effect on the composition of the bone after ovariectomy and most of this effect appears to be in the protein phase rather than reverting the mineral to protein ratio. Combining this relative compositional data from Raman with the micro CT results, which provide insight into the absolute volume of bone mineral informs us that although all three treatments yielded a maintenance of bone mass within levels not significantly different to the sham samples, the composition of the bone after each treatment is significantly different.

Overall the analysis of the data shows that while the interventions vary in their efficacy at maintaining physiological bone structure, their protective effect is stronger on the proteins than the mineral phase. Protective effects on the protein phase include preventing formation of random protein structure, reducing free acid side chains and maintaining hydrophilicity of chain for bioavailability. ALN and PTH also reduced the amount of mineral loss (relative to protein) to approximately half, but E2 had no significant effect. The interventions also vary in the nature and quantity of the non-physiological structural changes such as inducing globular alpha helices and beta sheet conformation. There is a considerable amount of protein level changes consequent upon application of each regime that is poorly understood. Most of the investigation into the mechanism of action of these drugs has focused on BMD. These data, combined with the authors recent publications [9, 10], make it clear that there is considerable influence that protein structure has on bone health. The authors would contend that the data illustrates an urgent and compelling need to more comprehensively examine the contribution of structural proteins to bone health and the impact of the methods commonly used to try ameliorating the risk of fracture.

4.2 Analysis of effects of anti-osteoporotic treatments on claws

The data presented suggests that both treatment with the ALN and PTH prevent significant changes in the nail keratin, however, significant changes were observed in the E2 treated group, largely aligned with the changes observed upon ovariectomy. The lack of protective effect on composition from E2 is surprising taking into account its complete reversal of body weight gain and loss of both trabecular and cortical bone by ovariectomy. In all three treatments the pattern of effects due to treating ovariectomised tissue exhibit very similar trends between bone and claw for each treatment model. For the OVX vs OVX-A model the sham, OVX-A and OVX-P groups are positive, while OVX and OVX-E2 are negative and the same applies for the OVX vs OVX-P model. While the discriminatory power of the OVX vs OVX-E2 models is weaker, the only difference between the two tissues is that OVX-A differs

but exhibits very large error bars in the bone indicating a very large amount of uncertainty in this group. Comparing the discriminant functions between the two tissues is restricted to the non-mineral region of the spectrum and here we see broad similarities between the two tissues, especially in the region sensitive to protein secondary structure.

4.3 Concluding remark

The authors have recently shown ovariectomy can induce changes to bone and keratin structure in a similar concurrent manner. The present study has demonstrated that treatment with three anti-osteoporotic pharmaceutical agents used in the clinic influenced the structure of bone collagen and claw keratin post-ovariectomy in rat. Mineral factors such as relative mineral to protein content were less strongly affected. It is notable that each treatment affected the protein phase of the bone differently. A better understanding of the protein status could therefore provide a better insight into an appropriate treatment to counteract the specific protein deficiencies within a specific patient. The changes in keratin are not as dramatic as observed in the bone collagen but have been shown to nevertheless act as useful surrogate markers of the bone remodelling under treatment with ALN and PTH. Thus, Raman spectroscopy measurement of keratinous tissue could be of value in monitoring the response to bone anabolic and anti-resorptive therapy of osteoporosis.

4.4 Limitations and further work

Unlike bone, once the claw tissue is formed it is no longer a living tissue and will no longer be significantly impacted by systemic changes. Further research is needed into the sampling patterns associated with different growth intervals to allow differentiation of pre- and post-intervention areas of the claw. This would be expected to improve sensitivity of the method.

It is not within the scope of this work to interpret the precise molecular implications of the differences beyond observing that

1. ALN is the closest to reverting the effects of ovariectomy.
2. Parathyroid hormone induces an extra change to the composition of the bone protein and mineral
3. E2, while allowing bone tissue volume to survive, yields bone tissue with a composition similar to that of untreated ovariectomised rats.

Studies designed to supplement the Raman data with additional independent methods of chemical and structural

analysis will help to elucidate these changes in more detail, especially for determining what factors are causative and which are correlative. For example, does the collagen deform thereby affecting its interactions with the mineral phase, or does the mineral phase change inducing structural deformation in the collagen? Furthermore, it would be important to establish how these compositional changes are related to the morphological changes observed.

Compliance with ethical standards

Conflict of interest RB and MCC are former employees of Crescent Ops Ltd, a company which owns intellectual property on the relationship between Raman spectroscopy, nail structure and fracture risk. MT and RB are shareholders in Crescent Ops Ltd. MT, NC, OOD and RB have served as consultants for Crescent Ops Ltd. Crescent Diagnostics Ltd funded the work carried out by MCC, JRB, (OD), NMC, MT and SHR. AI and AS declare no conflict of interest.

Publisher's note: Springer Nature remains neutral with regard to jurisdictional claims in published maps and institutional affiliations.

References

1. NIH Consensus Development Panel on Osteoporosis Prevention, Diagnosis, and Therapy. Osteoporosis prevention, diagnosis, and therapy. JAMA 2001;285:785–95. https://doi.org/10.1001/jama.285.6.785

2. Viguet-Carrin S, Garnero P, Delmas PD. The role of collagen in bone strength. Osteoporos Int. 2006;17:319–36. https://doi.org/10.1007/s00198-005-2035-9

3. Cummins NM, Day JCC, Wren A, Carroll P, Murphy N, Jakeman PM et al. Raman spectroscopy of fingernails: a novel tool for evaluation of bone quality? Spectroscopy. 2010;24:517–24. https://doi.org/10.3233/SPE-2010-0471

4. Towler MR, Wren A, Rushe N, Saunders J, Cummins NM, Jakeman PM. Raman spectroscopy of the human nail: a potential tool for evaluating bone health? J Mater Sci Mater Med. 2007;18:759–63. https://doi.org/10.1007/s10856-006-0018-9

5. Moran P, Towler MR, Chowdhury S, Saunders J, German MJ, Lawson NS et al. Preliminary work on the development of a novel detection method for osteoporosis. J Mater Sci Mater Med. 2007;18:969–74. https://doi.org/10.1007/s10856-006-0037-6

6. Pillay I, Lyons D, German MJ, Lawson NS, Pollock HM, Saunders J et al. The use of fingernails as a means of assessing bone health: a pilot study. J Women's Health (Larchmt). 2005;14:339–44. https://doi.org/10.1089/jwh.2005.14.339

7. Beattie JR, Cummins NM, Caraher C, O'Driscoll OM, Bansal AT, Eastell R et al. Raman spectroscopic analysis of fingernail clippings can help differentiate between postmenopausal women who have and have not suffered a fracture. Clin Med Insights Arthritis Musculoskelet Disord. 2016;9:109–16. https://doi.org/10.4137/CMAMD.S38493

8. Beattie JR, Caraher MC, Cummins NM, O'Driscoll OM, Eastell R, Ralston SH et al. Raman spectral variation for human fingernails of postmenopausal women is dependent on fracture risk and osteoporosis status. J Raman Spectrosc. 2017;48:813–21. https://doi.org/10.1002/jrs.5123

9. Beattie JR, Feskanich D, Caraher MC, Towler MR. A preliminary evaluation of the ability of keratotic tissue to act as a prognostic indicator of hip fracture risk. Clin Med Insights Arthritis Musculoskelet Disord. 2018;11:117954411775405 https://doi.org/10.1177/1179544117754050

10. Caraher MC, Sophocleous A, Beattie JR, O'Driscoll O, Cummins NM, Brennan O et al. Raman spectroscopy predicts the link between claw keratin and bone collagen structure in a mouse model of oestrogen deficiency. Biochim Biophisica Acta Mol Basis Dis. 2018;1864:398–406.

11. Bruyere O, Roux C, Detilleux J, Slosman DO, Spector TD, Fardellone P et al. Relationship between bone mineral density changes and fracture risk reduction in patients treated with strontium ranelate. J Clin Endocrinol Metab. 2007;92:3076–81. https://doi.org/10.1210/jc.2006-2758

12. Cummings SR, Karpf DB, Harris F, Genant HK, Ensrud K, LaCroix AZ et al. Improvement in spine bone density and reduction in risk of vertebral fractures during treatment with antiresorptive drugs. Am J Med. 2002;112:281–9. https://doi.org/10.1016/S0002-9343(01)01124-X

13. Guo R-T, Cao R, Liang P-H, Ko T-P, Chang T-H, Hudock MP et al. Bisphosphonates target multiple sites in both cis- and transprenyltransferases. Proc Natl Acad Sci USA. 2007;104:10022–7. https://doi.org/10.1073/pnas.0702254104

14. Liberman UA, Weiss SR, Bröll J, Minne HW, Quan H, Bell NH et al. Effect of oral alendronate on bone mineral density and the incidence of fractures in postmenopausal osteoporosis. N Engl J Med. 1995;333:1437–44. https://doi.org/10.1056/NEJM199511303332201

15. Black DM, Thompson DE, Bauer DC, Ensrud K, Musliner T, Hochberg MC et al. Fracture risk reduction with alendronate in women with osteoporosis: the fracture intervention trial. J Clin Endocrinol Metab. 2000;85:4118–24. https://doi.org/10.1210/jcem.85.11.6953

16. Black DM, Cummings SR, Karpf DB, Cauley JA, Thompson DE, Nevitt MC et al. Randomised trial of effect of alendronate on risk of fracture in women with existing vertebral fractures. Lancet. 1996;348:1535–41. https://doi.org/10.1016/S0140-6736(96)07088-2

17. Cummings SR, Black DM, Thompson DE, Applegate WB, Barrett-Connor E, Musliner TA et al. Effect of alendronate on risk of fracture in women with low bone density but without vertebral fractures: results from the fracture intervention trial. JAMA. 1998;280:2077 https://doi.org/10.1001/jama.280.24.2077

18. Cauley JA, Seeley DG, Ensrud K, Ettinger B, Black D, Cummings SR. Estrogen replacement therapy and fractures in older women. Ann Intern Med. 1995;122:9 https://doi.org/10.7326/0003-4819-122-1-199501010-00002

19. Khajuria DK, Razdan R, Mahapatra DR. Drugs for the management of osteoporosis: a review. Rev Bras Reumatol. 2011;51:372–82. https://doi.org/10.1590/S0482-50042011000400008

20. Dede AD, Makras P, Anastasilakis AD. Investigational anabolic agents for the treatment of osteoporosis: an update on recent developments. Expert Opin Investig Drugs. 2017;26:1137–44. https://doi.org/10.1080/13543784.2017.1371136

21. Neer RM, Arnaud CD, Zanchetta JR, Prince R, Gaich GA, Reginster J-Y et al. Effect of parathyroid Hormone (1-34) on fractures and bone mineral density in postmenopausal women with osteoporosis. N Engl J Med. 2001;344:1434–41. https://doi.org/10.1056/NEJM200105103441904

22. Trevisani VFM, Riera R, Imoto AM, Saconato H, Atallah ÁN. Teriparatide (recombinant human parathyroid hormone 1-34) in postmenopausal women with osteoporosis: systematic review. Sao Paulo Med J. 2008;126:279–84. https://doi.org/10.1590/S1516-31802008000500007.

23. A Sophocleous, AI Idris, Rodent models of osteoporosis, Bonekey Rep. 3 (2014). https://doi.org/10.1038/bonekey.2014.109

24. Beattie JR. Optimising reproducibility in low quality signals without smoothing; an alternative paradigm for signal processing. J Raman Spectrosc. 2011;42:1419–27. https://doi.org/10.1002/jrs.2851

25. Beattie JR, McGarvey JJ. Estimation of signal backgrounds on multivariate loadings improves model generation in face of complex variation in backgrounds and constituents. J Raman Spectrosc. 2013;44:329–38. https://doi.org/10.1002/jrs.4178

26. Beattie JR, Glenn JV, Boulton ME, Stitt AW, McGarvey JJ. Effect of signal intensity normalization on the multivariate analysis of spectral data in complex "real-world" datasets. J Raman Spectrosc. 2009;40:429–35. https://doi.org/10.1002/jrs.2146

27. Palacký J, Mojzeš P, Bok J. SVD-based method for intensity normalization, background correction and solvent subtraction in Raman spectroscopy exploiting the properties of water stretching vibrations. J Raman Spectrosc. 2011;42:1528–39. https://doi.org/10.1002/jrs.2896

28. Mandair GS, Esmonde-White FWL, Akhter MP, Swift AM, Kreider J, Goldstein SA et al. Potential of Raman spectroscopy for evaluation of bone quality in osteoporosis patients: results of a prospective study, In: Kollias N, Choi B, Zeng H, Malek RS, Wong BJ, Ilgner JFR (eds). USA: International Society for Optics and Photonics; 2010: p. 754846. https://doi.org/10.1117/12.842515

29. Penel G, Delfosse C, Descamps M, Leroy G. Composition of bone and apatitic biomaterials as revealed by intravital Raman microspectroscopy. Bone. 2005;36:893–901. https://doi.org/10.1016/j.bone.2005.02.012

30. Campbell GM, Sophocleous A, Quantitative analysis of bone and soft tissue by micro-computed tomography: applications to ex vivo and in vivo studies, Bonekey Rep. 3 (2014). https://doi.org/10.1038/bonekey.2014.59

31. Papapoulos SE, Quandt SA, Liberman UA, Hochberg MC, Thompson DE. Meta-analysis of the efficacy of alendronate for the prevention of hip fractures in postmenopausal women. Osteoporos Int. 2005;16:468–74. https://doi.org/10.1007/s00198-004-1725-z

32. Lindsay R, Gallagher JC, Kagan R, Pickar JH, Constantine G. Efficacy of tissue-selective estrogen complex of bazedoxifene/conjugated estrogens for osteoporosis prevention in at-risk postmenopausal women. Fertil Steril. 2009;92:1045–52. https://doi.org/10.1016/J.FERTNSTERT.2009.02.093

33. Hodsman AB, Hanley DA, Ettinger MP, Bolognese MA, Fox J, Metcalfe AJ et al. Efficacy and safety of human parathyroid Hormone-(1–84) in increasing bone mineral density in postmenopausal osteoporosis. J Clin Endocrinol Metab. 2003;88:5212–20. https://doi.org/10.1210/jc.2003-030768

34. Cosman F, Combination therapy for osteoporosis: a reappraisal, Bonekey Rep. 3 (2014). https://doi.org/10.1038/bonekey.2014.13

35. Allen MR, Gineyts E, Leeming DJ, Burr DB, Delmas PD. Bisphosphonates alter trabecular bone collagen cross-linking and isomerization in beagle dog vertebra. Osteoporos Int. 2008;19:329–37. https://doi.org/10.1007/s00198-007-0533-7

36. Saito M, Marumo K, Kida Y, Ushiku C, Kato S, Takao-Kawabata R et al. Changes in the contents of enzymatic immature, mature, and non-enzymatic senescent cross-links of collagen after once-weekly treatment with human parathyroid hormone (1–34) for 18 months contribute to improvement of bone strength in ovariectomized monkeys. Osteoporos Int. 2011;22:2373–83. https://doi.org/10.1007/s00198-010-1454-4

37. Saito M, Marumo K. Collagen cross-links as a determinant of bone quality: a possible explanation for bone fragility in aging, osteoporosis, and diabetes mellitus. Osteoporos Int. 2010;21:195–214. https://doi.org/10.1007/s00198-009-1066-z

38. Boivin G, Chavassieux P, Santora A, Yates J, Meunier P. Alendronate increases bone strength by increasing the mean degree of mineralization of bone tissue in osteoporotic women. Bone. 2000;27:687–94. https://doi.org/10.1016/S8756-3282(00)00376-8

39. Boskey AL, Spevak L, Weinstein RS. Spectroscopic markers of bone quality in alendronate-treated postmenopausal women. Osteoporos Int. 2009;20:793–800. https://doi.org/10.1007/s00198-008-0725-9

40. Allen MR, Burr DB. Mineralization, microdamage, and matrix: how bisphosphonates influence material properties of bone. BoneKEy-Osteovision. 2007;44:49–6049. https://doi.org/10.1138/20060248

41. Tang SY, Allen MR, Phipps R, Burr DB, Vashishth D. Changes in non-enzymatic glycation and its association with altered mechanical properties following 1-year treatment with risedronate or alendronate. Osteoporos Int. 2009;20:887–94. https://doi.org/10.1007/s00198-008-0754-4

42. Paschalis E, Boskey A, Kassem M, Eriksen E. Effect of hormone replacement therapy on bone quality in early postmenopausal women. J Bone Miner Res. 2003;18:955–9. https://doi.org/10.1359/jbmr.2003.18.6.955

43. Ascenzi M-G, Liao VP, Lee BM, Billi F, Zhou H, Lindsay R et al. Parathyroid hormone treatment improves the cortical bone microstructure by improving the distribution of type I collagen in postmenopausal women with osteoporosis. J Bone Miner Res. 2012;27:702–12. https://doi.org/10.1002/jbmr.1497

44. Morris MD, Mandair GS. Raman assessment of bone quality. Clin Orthop Relat Res. 2011;469:2160–9. https://doi.org/10.1007/s11999-010-1692-y

45. Widjaja E, Lim GH, An A. A novel method for human gender classification using Raman spectroscopy of fingernail clippings. Analyst. 2008;133:493 https://doi.org/10.1039/b712389b

46. Garland M, Morris JS, Stampfer MJ, Colditz GA, Spate VL, Baskett CK et al. Prospective study of toenail selenium levels and cancer among women. JNCI J Natl Cancer Inst. 1995;87:497–505. https://doi.org/10.1093/jnci/87.7.497

47. Pelton JT, McLean L. Spectroscopic methods for analysis of protein secondary structure. Anal Biochem. 2000;277:167–76. https://doi.org/10.1006/ABIO.1999.4320